A cobalt(II)-nitronyl nitroxide single chain magnet with a record high blocking temperature and low coercivity†

Thomaz de A. Costa[a], Mihai Răducă[b,c], Julio C. Rocha[a,d], Miguel A. Novak[e], Rafael A. A. Cassaro[f]*, Marius Andruh[b,c]* and Maria G. F. Vaz[a,]*

[a] *Instituto de Química, Universidade Federal Fluminense, Niterói, 24020-150, RJ, Brazil;*
[b] *Inorganic Chemistry Laboratory, Faculty of Chemistry, University of Bucharest, Bd. Regina Elisabeta 4-12, 030018-Bucharest, Romania*
[c] *"C. D. Nenitzescu" Institute of Organic and Supramolecular Chemistry of the Romanian Academy, Splaiul Independentei 202 B, 060023-Bucuarest, Romania*
[d] *Departamento de Farmácia, Faculdade de Ciências Biológicas e da Saúde, Universidade do Estado do Rio de Janeiro, 23070-200, Rio de Janeiro-RJ, Brasil*
[e] *Instituto de Física, Universidade Federal Fluminense, Niterói, 24210-240, RJ, Brazil*
[f] *Instituto de Química, Universidade Federal do Rio de Janeiro, 21941-909, RJ, Brazil;*
**allao.cassaro@iq.ufrj.br*
**marius.andruh@acad.ro*
**mariavaz@id.uff.br*

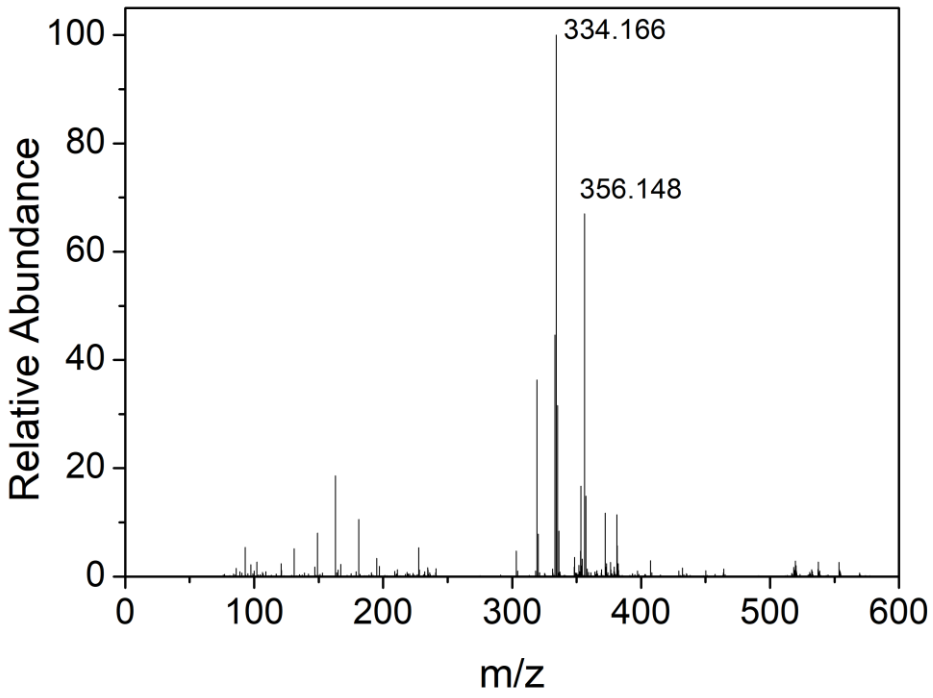

Figure S1: High-resolution mass spectrometry for 9-PhentNIT.

Table S1: Crystallographic data and structure refinement for **1** and **2**.

Compound	**1**	**2**
Chemical formula	$C_{31}H_{23}N_2F_{12}O_6Mn$	$C_{31}H_{23}N_2F_{12}O_6Co$
M (g mol^{-1})	802.44	806.44
Temperature, (K)	100(1)	110(5)
Wavelength, (Å)	0.67018	0.67018
Crystal system	*Monoclinic*	*Monoclinic*
Space group	*P2$_1$/n*	*P2$_1$/n*
a (Å)	23.526(17)	23.179(10)
b (Å)	13.451(9)	13.712(8)
c (Å)	24.162(15)	23.894(8)
α (º)	90	90
β (º)	113.970(6)	113.409(10)
γ (º)	90	90
V (Å^3)	6987(8)	6969(6)
Z	4	4
D_c (g cm^{-3})	1.526	1.537
μ (mm^{-1})	0.416	0.516
F(000)	3232	3248
θ range (deg.)	1.6-23.811	1.621-24.119
Index range	-28≤h≤28 -16≤k≤16 -28≤l≤28	-28≤h≤28 -16≤k≤16 -28≤l≤28
Data collected/ Independent reflections	83193/12756 [R_{int}=0.1111]	84611/13150[R_{int}=0.0787]
Data / restraints / parameters	12756/119/867	13150/132/905
GOF	1.038	1.043
Final R_1, wR_2 [I>2σ(I)]	0.0954, 0.2712	0.0818, 0.2267
R_1, wR_2 (all data)	0.1571, 0.3269	0.1097, 0.2552
$\Delta\rho_{min}/\Delta\rho_{max}$ (e Å^{-3})	1.228, -0.617	1.237, -0.932

Table S2: Analysis of coordination environment of manganese(II) and cobalt(II) ions for **1** and **2**, respectively.

Compound	**Metal**	**Oh**	**TPR-6**	**PPY-6**	**JPPY-6**	**HP-6**
1	Mn1	2.64	7.08	20.6	24.2	31.0
	Mn2	3.26	5.98	20.3	24.0	31.8
2	Co1	1.42	9.47	23.5	27.1	30.9
	Co2	1.15	10.3	23.6	27.2	30.3

Oh = Octahedron, TPR-6 = Trigonal prism, PPY-6 = Pentagonal pyramid, JPPY-6 = Johnson pentagonal pyramid J2, HP-6 = Hexagon.

Table S3: Distortion parameters calculated from the octahedron for **1** and **2**.

Compound	Metal	d_{mean} (Å)	ζ	Σ (º)	Θ (º)	V (Å^3)
1	Mn1	2.14	0.118	93.8	427	12.5
	Mn2	2.14	0.139	99.1	369	12.4
2	Co1	2.07	0.0715	70.8	265	11.5
	Co2	2.06	0.0742	66.0	230	11.5

Table S4: Selected bond lengths and bond angles for **1**. *Symmetry operation: 1-x,-1/2+y,3/2-z

Bond lengths (Å)			
Mn1-O1	2.100(5)	Mn2-O7	2.103(5)
Mn1-O2a*	2.118(5)	Mn2-O8a*	2.115(5)
Mn1-O3	2.155(5)	Mn2-O9	2.166(6)
Mn1-O4	2.151(5)	Mn2-O10	2.156(5)
Mn1-O5	2.167(5)	Mn2-O11	2.163(5)
Mn1-O6	2.138(5)	Mn2-O12	2.161(7)
Bond angles (º)			
O1-Mn1-O2a*	81.64(17)	O7-Mn2-O8a*	81.7(2)
O1-Mn1-O3	163.53(18)	O7-Mn2-O9	162.6(2)
O1-Mn1-O4	86.10(19)	O7-Mn2-O10	86.0(2)
O1-Mn1-O5	91.64(18)	O7-Mn2-O11	89.9(2)
O1-Mn1-O6	110.40(18)	O7-Mn2-O12	112.6(2)
O2a*-Mn1-O3	92.26(17)	O8a*-Mn2-O9	90.5(2)
O2a*-Mn1-O4	108.91(18)	O8a*-Mn2-O10	110.1(2)
O2a*-Mn1-O5	163.92(18)	O8a*-Mn2-O11	162.9(2)
O2a*-Mn1-O6	87.70(18)	O8a*-Mn2-O12	88.8(2)
O3-Mn1-O4	81.41(18)	O9-Mn2-O10	81.1(2)
O3-Mn1-O5	97.90(18)	O9-Mn2-O11	101.7(2)
O3-Mn1-O6	84.47(18)	O9-Mn2-O12	83.6(2)
O4-Mn1-O5	85.03(18)	O10-Mn2-O11	83.9(2)
O4-Mn1-O6	158.50(17)	O10-Mn2-O12	155.63(18)
O5-Mn1-O6	80.94(18)	O11-Mn2-O12	80.7(2)

Table S5: Short contact distances between fluorine atoms for **2**. *Refers to a fluorine atom originating from disorder

F···F(Å)	
Compound	**2**
F1···F14	3.120(30)
F8···F13a*	2.956(15)
F8···F22	3.050(8)

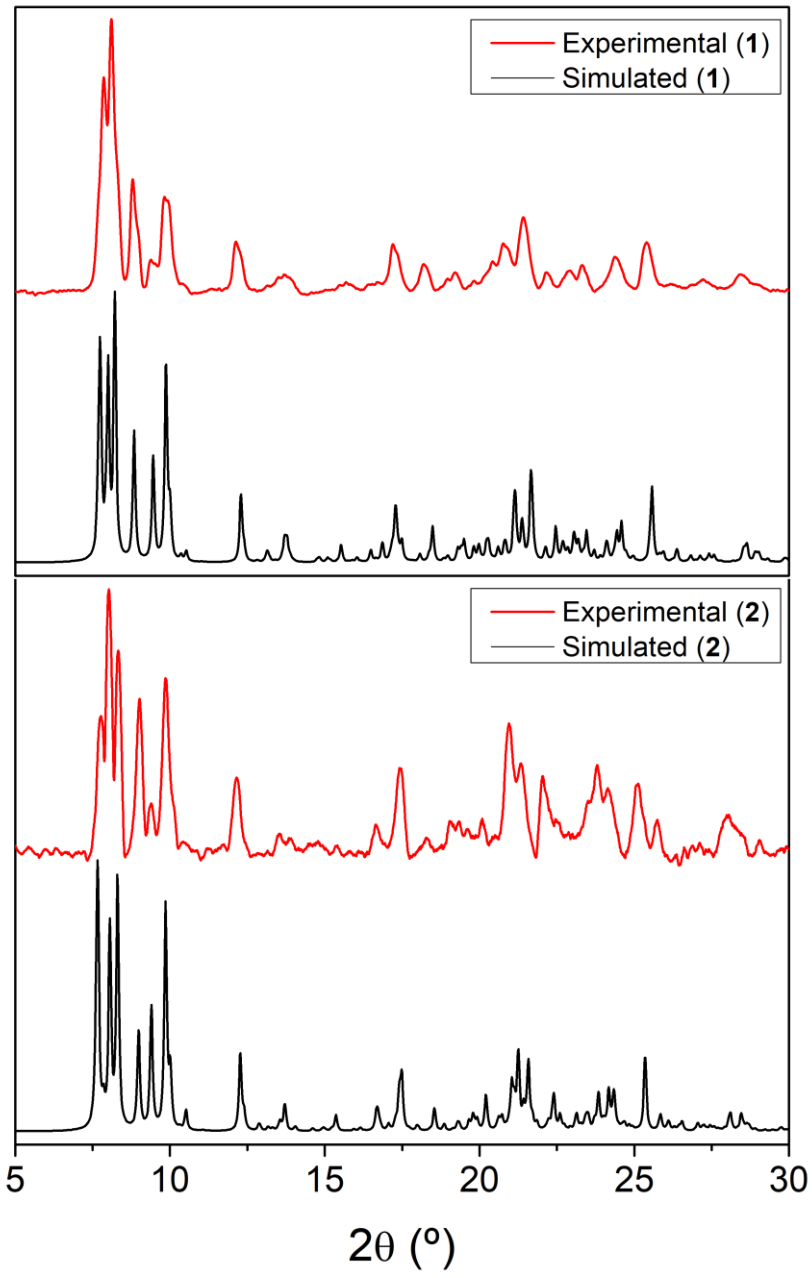

Figure S2: Simulated and experimental powder X-ray diffraction patterns for **1** and **2**.

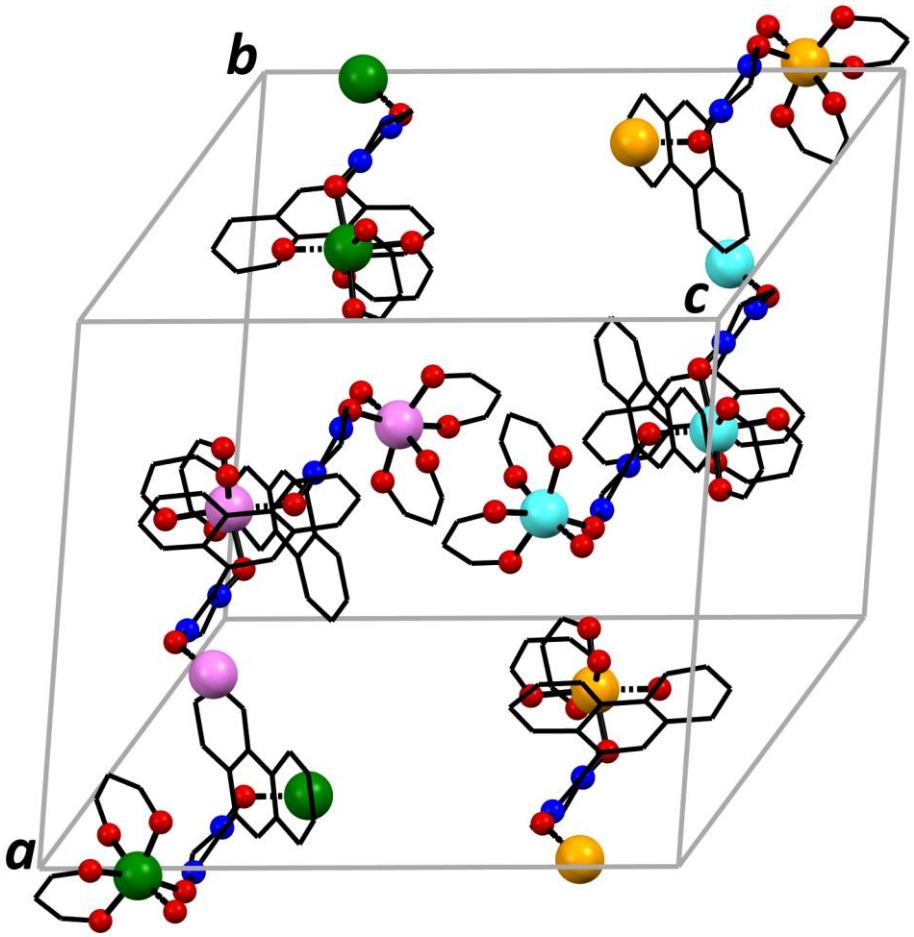

Figure S3: View of the unit cell of compound ***2***. Enantiomeric atoms: Pink (Co1/Δ), cyan (Co1/Λ), green (Co2/Δ) and orange (Co2/Λ). Atoms: carbon (black), nitrogen (blue) and oxygen (red). Methyl groups, hydrogen, and fluorine atoms were omitted for clarity.

Fit of magnetic susceptibility of 1

$$H = -J\sum S_I . S_{i+1} \tag{S1}$$

$$\chi_M T = \frac{N\mu_B^2}{k_B}\left\{\begin{array}{c} g_{Mn}^2 S_{Mn}^2\left(\frac{S_{Mn}+1}{S_{Mn}} + \frac{2\delta}{1-\delta}\right) - 4g_{Mn}g_R\Lambda S_{Mn}S_R\frac{1}{1-\delta} + \\ g_R^2(S_R(S_R+1) + 2\Lambda^2 S_R^2\frac{1}{1-\delta}) \end{array}\right\} \tag{S2}$$

With:

$$\gamma = -\frac{JS_{Mn}}{k_B T}$$

$$a_0 = 4(\gamma^{-1}\, senh\,\gamma - \gamma^{-2}\cos\gamma + \gamma^{-2})$$

$$a_1 = 12[(\gamma^{-1} + 12\gamma^{-3}) senh\,\gamma - (5\gamma^{-2} + 12\gamma^{-4})\cosh\gamma - \gamma^{-2} + 12\gamma^{-4}]$$

$$b_0 = \gamma^{-1}(\cosh\gamma - 1)$$

$$b_1 = 3[(\gamma^{-1} + 4\gamma^{-3})\cosh\gamma - 4\gamma^{-2} senh\,\gamma + \gamma^{-1} - 4\gamma^{-3}]$$

$$\delta = \frac{a_1}{3a_0}$$

$$\Lambda = 2\left(\frac{b_1}{3a_0} + \frac{b_0}{a_0}\right)$$

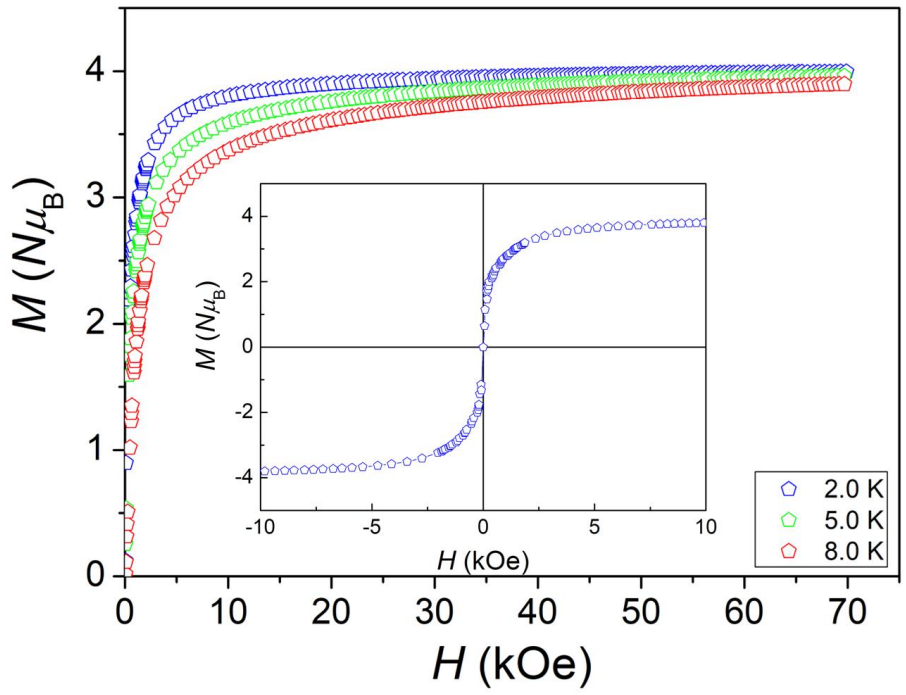

Figure S4: Field dependence of magnetization at different temperatures for **1** with the inset highlighting the absence of hysteresis

Table S6: Geometrical parameters and J values for selected Mn(II)-Nit chains.

Compound	$J_{Mn\text{-}NIT}$ (cm^{-1})	Mn-O (Å)	O-Mn-O (º)	Mn-O-N (°)	Mn-O-N-C (°)	Ref.
$Mn(hfac)_2NITPhOMe$[a]	-344	2.143 (5) 2.121 (5)	86.9(2)	131.1 (5) 127.4 (5)	89.5 (9) 87.6 (8)	3
$[Mn(hfac)_2NIT(Ph\text{-}m\text{-}OPh)]$[b]	-220	2.142 (3) 2.142 (3)	88.1(1)	126.8(2) 123.7(2)	76.7(4) 75.3(4)	4
$[Mn(hfac)_2(NaphNN)]_n$[c]	-298	2.125(4) 2.089(4)	85.3(2)	124.6(3) 128.8(3)	-84.5(5) -87.0(5)	5
$[Mn(hfac)_2(pyrNN)]$[d]	-275	2.100(8) 2.106(8)	81.7(3)	126.7(7) 123.0(7)	77.8(13) 76.2(14)	6
$[Mn(hfac)_2(9\text{-}PhentNIT)]_n$	-238	2.100(5) 2.118(5) 2.103(5) 2.115(5)	81.6(2) 81.7(2)	125.1(4) 123.4(3) 125.9(4) 124.0(4)	72.0(7) 72.1(8) 71.6(8) 71.3(9)	This work

[a]NITPhOMe = 2-(4-methoxyphenyl)-4,4,5,5-tetramethylimidazoline-1-oxyl 3-oxide, [b]NIT(Ph-m-OPh) = 3-(1-Phenoxybenzene)-4,4,5,5-tetramethylimidazoline-1-oxyl-3-oxide, [c]NaphNN = 2-(1′-naphthalenyl)-4,4,5,5-tetramethyl-4,5-dihydro-1H-imidazole-3-oxide-1-oxyl, [d]pyrNN = 2-(1′pyrenyl)-4,4,5,5-tetramethyl-4,5-dihydro-1H-imidazole-3-oxide1-oxyl.

Fit of magnetic susceptibility of 2

The χT *vs* T data was fitted using the branch chain (Eq. S4) model, where $\mathbf{S_{Co}}$ = 3/2 and $\mathbf{S_R}$ = ½, using the Hamiltonian described by Eq. S3.

$$H = \sum_{I} \begin{Bmatrix} -J\left[S_{Co,i,(z)}.\left(S_{R,i(z)} + S_{R,i-1(z)}\right)\right] + J_a L_{Co,i,(z)} S_{Co,i,(z)} + D L_{Co,i,(z)}{}^2 \\ -\mu_B H(g_{Co} S_{Co,i,(z)} + g_R S_{R,i(z)} + k L_{Co,i,(z)} \end{Bmatrix} \quad \text{(S3)}$$

$$\chi T = \frac{N\mu_B^2}{k_B}\left[\frac{u^2 a + 2uc + \frac{(ua+c)^2}{b} + d}{a+b}\right] \quad \text{(S4)}$$

With:

$$a = (2e^z \cosh 3y + 1)\cosh 6x + (2e^z \cosh y + 1)\cosh 2x$$

$$b = 2[e^z(\cosh 3y + \cosh y) + 1$$

$$c = \{e^z[e^{-3y}(3v-k) + e^{3y}(3v+k)] + 3v\}\text{senh } 6x + \left[e^z\left(e^{-y}(v-k)\right) + e^y(v+k) + v\right]\text{senh } 2x$$

$$d = \{e^z[e^{-3y}(3v-k)^2 + e^{3y}(3v+k)^2] + (3v)^2\}(1+\cosh 6x) + \{e^z[e^{-y}(v-k)^2 + e^y(v+k)^2] + v^2\}(1+\cosh 2x)$$

$$u = \frac{g_R}{2}; \qquad v = \frac{g_{Co}}{2}; \qquad x = \frac{J}{4k_BT}; \qquad y = \frac{-J_a}{2k_BT}; \qquad z = \frac{-D}{k_BT}$$

J represents cobalt(II)-radical exchange interaction, β is the Bohr Magneton and *k* is covalency factor, k_B is Boltzmann´s constant, T is temperature and $\boldsymbol{g_R}$ and $\boldsymbol{g_{Co}}$ are the Landé factors for the radical and cobalt(II), respectively. J_a is the effective spin-orbit coupling, which can be related to the spin-orbit coupling parameter (λ) through the expression $J_a = -(3/2)k\lambda$.

The best fit parameters obtained were: J/k_B = –(253±10) K (–176±7 cm^{-1}), J_a/k_B = 216 K (150 cm^{-1}) fixed, D/k_B = –144 K (–100 cm^{-1}) fixed, $\boldsymbol{g}_{Co}$ = 2.9±0.3, $\boldsymbol{g_R}$ = 2.0 (fixed) and *k* = 0.7 (fixed) for $T \geq 69$ K. Some parameters were fixed to avoid overparametrization. The orbital reduction *k* was fixed to 0.7, a typical value observed for hexacoordinated cobalt(II) ions.[1] Using the *k* value (0.7) gives the spin-orbit coupling parameter λ= –143 cm^{-1}, not far to the value observed for cobalt(II) free ion[2] –180 cm^{-1}.

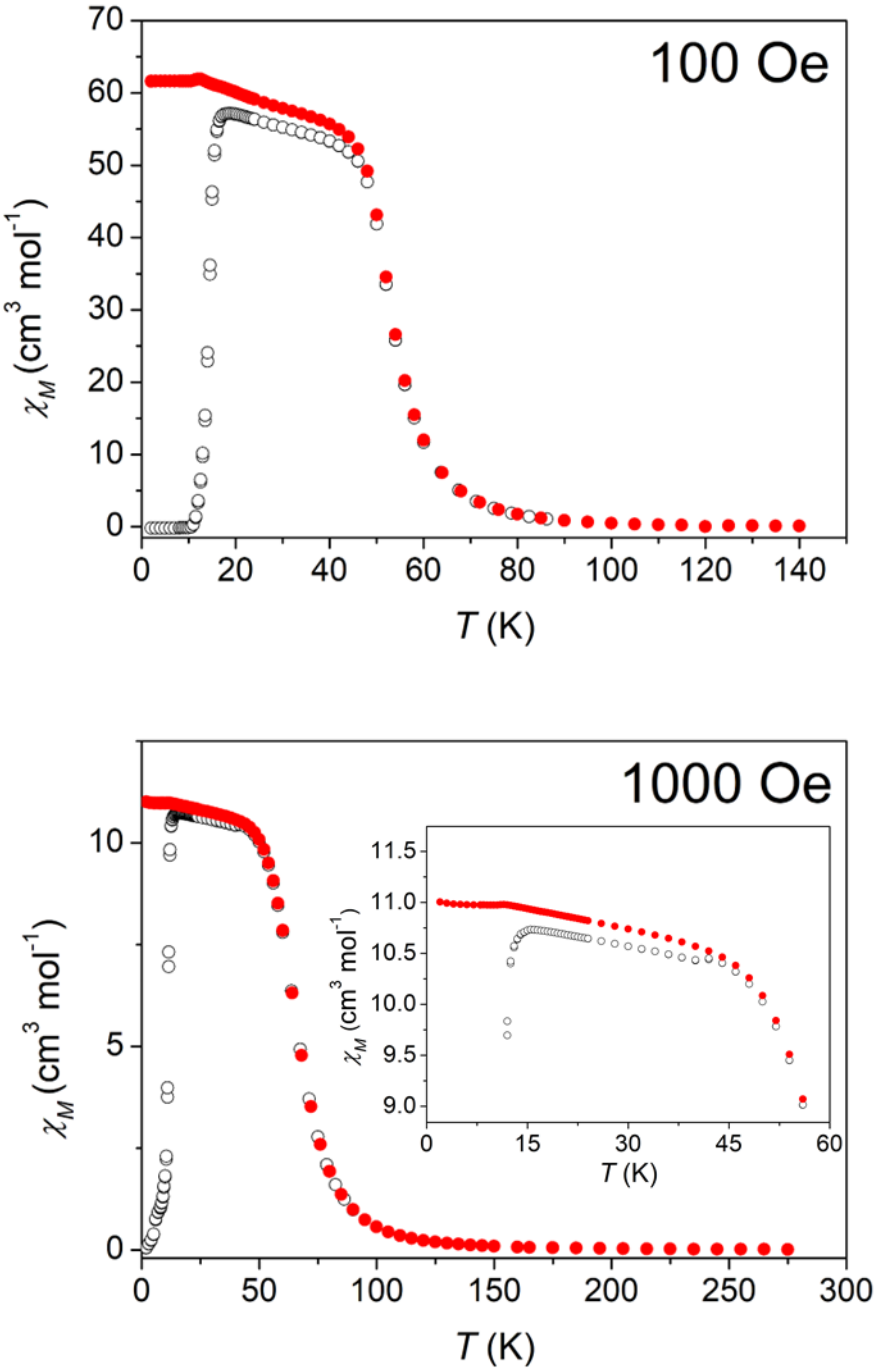

Figure S5: Temperature dependence of ZFC (black, open circles) and FC (red, filled circles) magnetic susceptibilities for **2** at 100 and 1000 Oe.

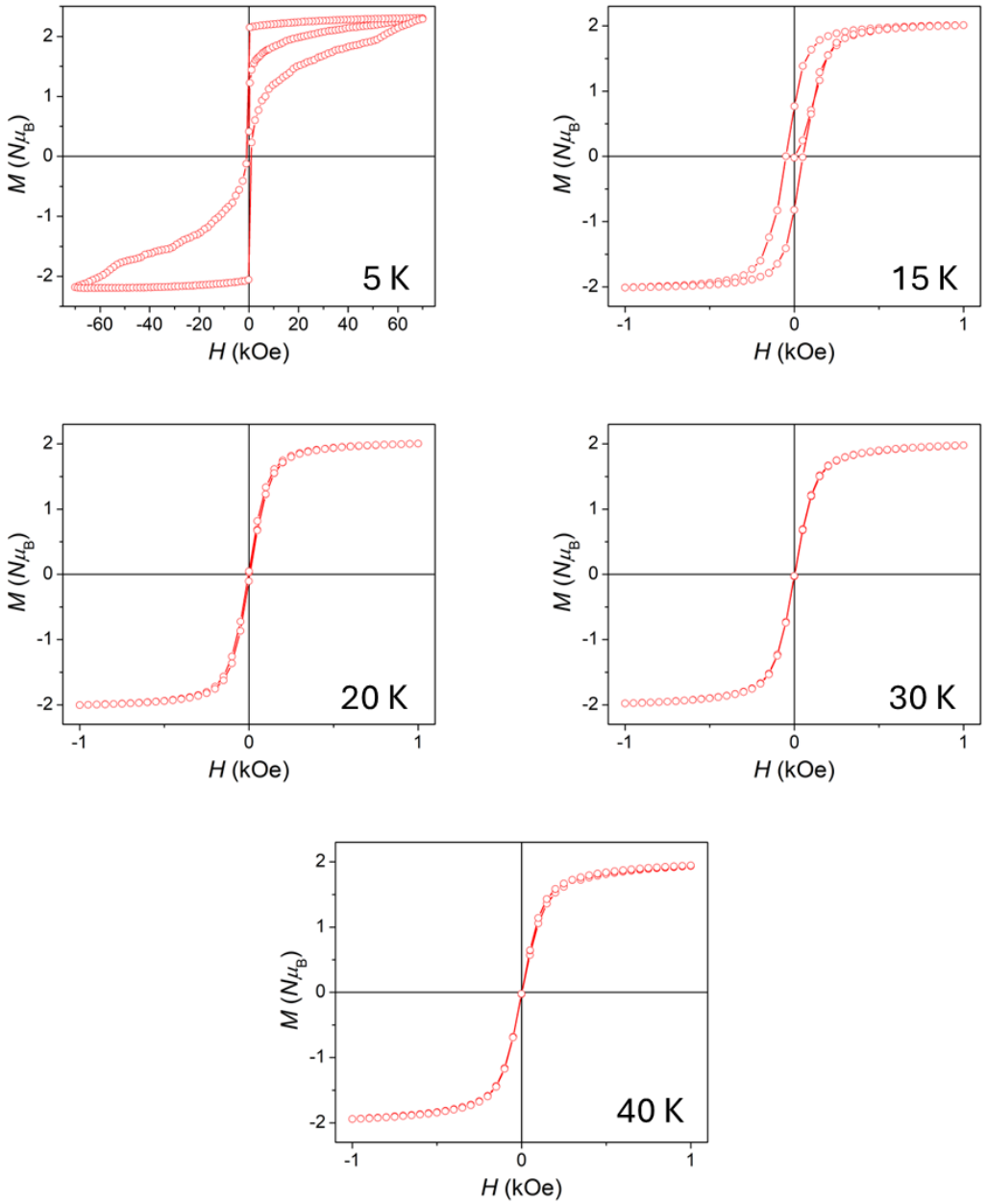

Figure S6: Field dependence of magnetization at different temperatures for **2**. At 5, 15 and 20 K hysteresis is observed

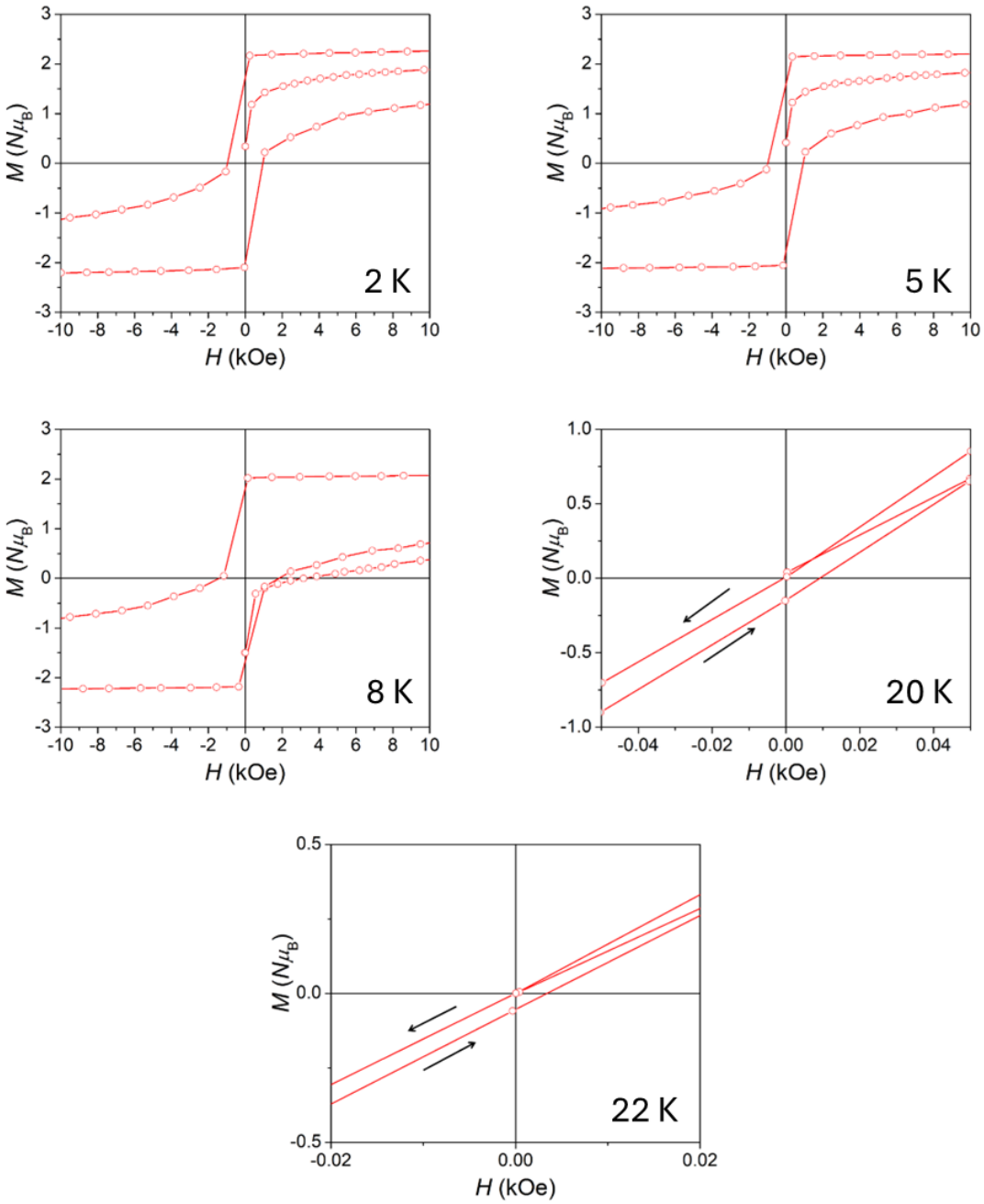

Figure S7: Hysteresis on an expanded scale

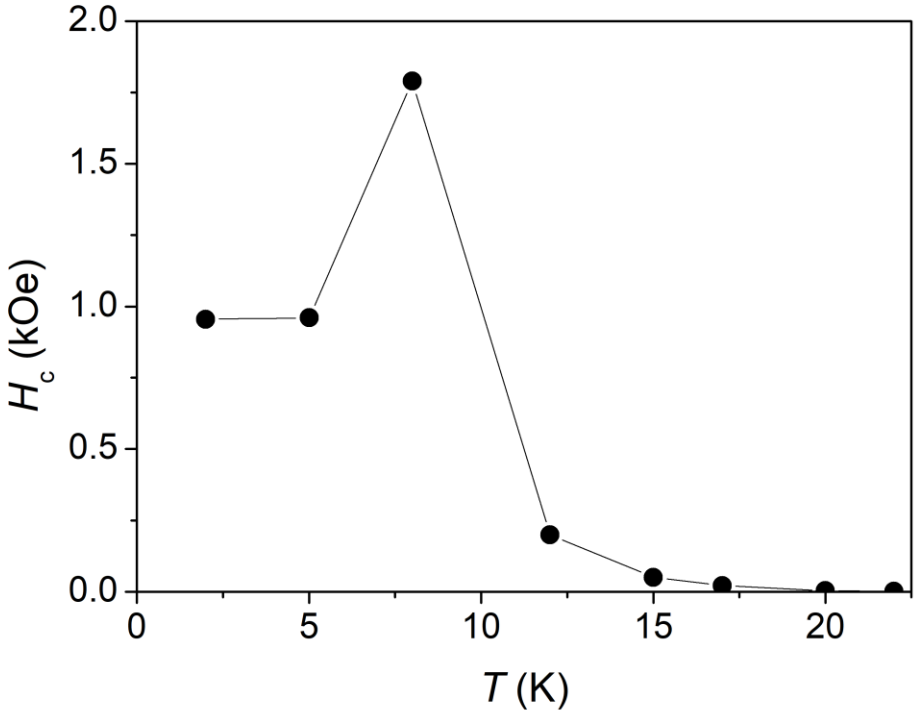

Figure S8: Evolution of the average coercive field with temperature

Treatment of ac magnetic susceptibility of 2

Isothermal frequency dependence of in phase (χ') and out of phase (χ'') magnetic susceptibilities were fitted using a sum of two Casimir and Duprè expression according to Eq. S6-Eq. S7.

$$\chi(\omega) = \chi_{S,A} + \chi_{S,B} + \frac{(\chi_T - \chi_s)_A}{1 + (i\omega\tau_A)^{1-\alpha_A}} + \frac{(\chi_T - \chi_s)_B}{1 + (i\omega\tau_B)^{1-\alpha_B}}$$

$$\chi_{S,total} = \chi_{S,A} + \chi_{S,B}$$

Eq. S5

$$\chi'(\omega) = \chi_{S,total} + (\chi_T - \chi_s)_A \frac{1 + (\omega\tau_A)^{1-\alpha_A} \sin(\pi \frac{\alpha_A}{2})}{1 + 2(\omega\tau_A)^{1-\alpha_A} \sin(\pi \frac{\alpha_A}{2}) + (\omega\tau_A)^{2-2\alpha_A}} + (\chi_T - \chi_s)_B \frac{(\omega\tau_B)^{1-\alpha_B} \sin(\pi \frac{\alpha_B}{2})}{1 + 2(\omega\tau_B)^{1-\alpha_B} \sin(\pi \frac{\alpha_B}{2}) + (\omega\tau_B)^{2-2\alpha_B}}$$

Eq. S6

$$\chi''(\omega) = (\chi_T - \chi_s)_A \frac{(\omega\tau_A)^{1-\alpha_A} \cos(\pi \frac{\alpha_A}{2})}{1 + 2(\omega\tau_A)^{1-\alpha_A} \sin(\pi \frac{\alpha_A}{2}) + (\omega\tau_A)^{2-2\alpha_A}} + (\chi_T - \chi_s)_B \frac{(\omega\tau_B)^{1-\alpha_B} \cos(\pi \frac{\alpha_B}{2})}{1 + 2(\omega\tau_B)^{1-\alpha_B} \sin(\pi \frac{\alpha_B}{2}) + (\omega\tau_B)^{2-2\alpha_B}}$$

Eq. S7

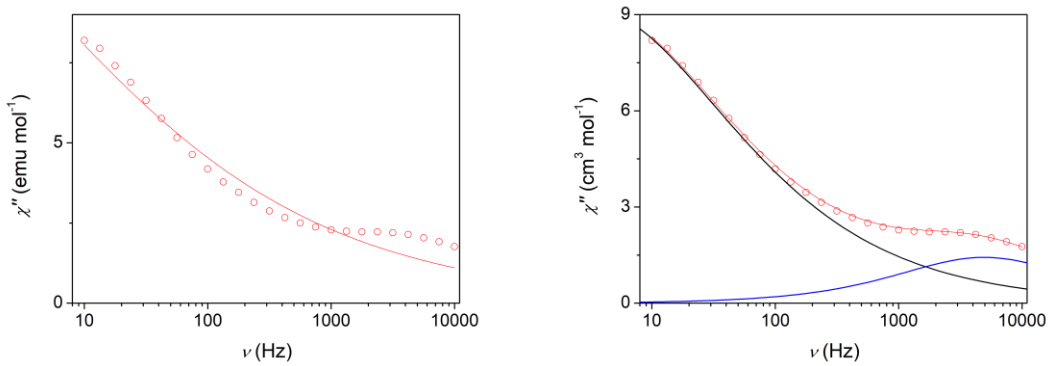

Figure S9: Frequency dependence of imaginary magnetic susceptibility at 25 K for **2** with the best fitted curves represented by red lines considering one relaxation process (left) and the sum of two relaxation processes (right). Black and blue lines represent the calculated curves for the **S** and **F** processes, respectively.

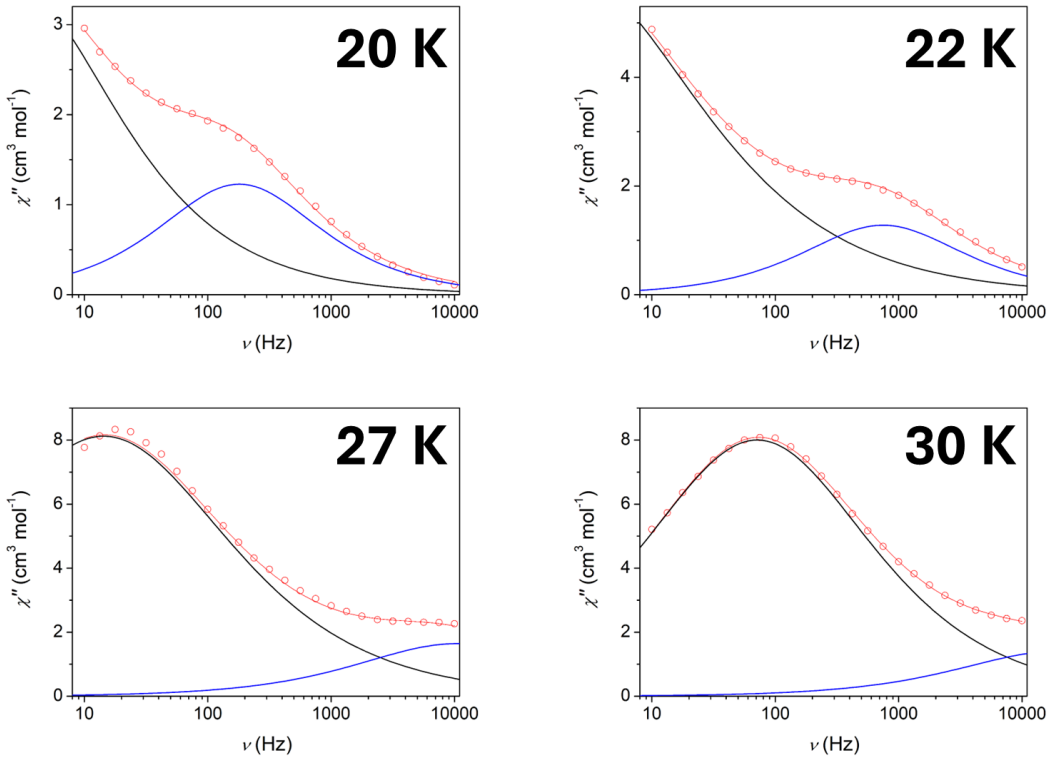

Figure S10: Frequency dependence of imaginary magnetic susceptibility at different temperatures. The red lines represent the sum of the two relaxation processes. Black and blue lines are the calculated curves for the contribution of **S** and **F** processes, respectively.

Table S7: Relaxation fitting parameters obtained using Eq. S6-S7 for **2**. These parameters were used to calculate the Cole-Cole plot.

T (K)	$(\chi_T-\chi_S)_1$ ($cm^3\ mol^{-1}$)	α_1	τ_1(s)	$(\chi_T-\chi_S)_2$ ($cm^3\ mol^{-1}$)	α_2	τ_2(s)
	F process			**S** process		
20	3.31	0.19	$9.85\cdot10^{-4}$	12.0	0.33	$6.51\cdot10^{-2}$
22	3.27	0.19	$2.02\cdot10^{-4}$	30.5	0.48	0.131
25	4.26	0.25	$3.22\cdot10^{-5}$	42.6	0.48	$5.12\cdot10^{-2}$
27	7.90	0.45	$8.93\cdot10^{-6}$	31.7	0.40	$1.10\cdot10^{-2}$
30	3.60	$7.8\cdot10^{-2}$	$5.81\cdot10^{-6}$	30.6	0.42	$2.16\cdot10^{-3}$
35	5.48	≈0	$1.09\cdot10^{-6}$	26.3	0.36	$2.07\cdot10^{-4}$
40	-	-	-	30.5	0.38	$1.37\cdot10^{-4}$
45	-	-	-	21.0	0.33	$1.87\cdot10^{-5}$

Table S8: Coercive fields at respective temperatures and blocking temperatures for the compounds for selected compounds

Compound	H_c | T (kOe | K)	T_B (K)	Ref.
$[Co(hfac)_2(NITPhOMe)]$[a]	10 | 2	-	7
$[Co(hfac)_2(PyrNN)]_n\cdot0.5cf\cdot0.5hep$ [b]	32 | 8	14	8
$[Co(hfac)_2(NaphNN)]_n$[c]	49 | 4	13.2	9
$Co(hfac)_2(MeONapNIT)$[d]	62 | 7	14	10
$Co(hfac)_2(EtONapNIT)$[d]	65 | 7	11	10
$[Co(hfac)_2PyrNN]_n\cdot0.5bf\cdot0.5hep$[b]	51 | 5	13.4	11
$[Co(hfac)_2L]_n$[e]	54 | 2	13	12
$[Co(hfac)_2(9\text{-}PhentNIT)]_n$	1.0 | 2	15.5	This work

[a]NITPhOMe = 2-(4-methoxyphenyl)-4,4,5,5-tetramethylimidazoline-1-oxyl 3-oxide, [b]pyrNN = 2-(1′pyrenyl)-4,4,5,5-tetramethyl-4,5-dihydro-1H-imidazole-3-oxide1-oxyl, [c]NaphNN = 2-(1′-naphthalenyl)-4,4,5,5-tetramethyl-4,5-dihydro-1H-imidazole-3-oxide-1-oxyl, [d]R-NapNIT = R-NapNIT = 2-(2′(R-)naphthyl)-4,4,5,5-tetramethylimidazoline-1-oxyl-3-oxide, R = MeO or EtO), [e]L = 2-ferrocenyl-4,4,5,5-tetramethyl-4,5-dihydro- 1H-imidazole-1-oxyl, cf = chloroform, bf = bromoform, hep = *n*-heptane.

1. F. Lloret, M. Julve, J. Cano, R. Ruiz-García and E. Pardo, Magnetic properties of six-coordinated high-spin cobalt(II) complexes: Theoretical background and its application, *Inorg. Chim. Acta*, 2008, **361**, 3432-3445.
2. R. L. Carlin and A. J. Van Duyneveldt, Magnetic Properties of Transition Metal Compounds, Spring-Verlag, New York, 1977, p.203.
3. A. Caneschi, D. Gatteschi, P. Rey and R. Sessoli, Structure and magnetic ordering of a ferrimagnetic helix formed by manganese(II) and a nitronyl nitroxide radical, *Inorg. Chem.*, 1991, **30**, 3936-3941.
4. X. Y. Qin, G. Xiong, D. Liao, Y. Ma, P. Gao, X. L. Sun and P. Liu, Synthesis, crystal structure, and magnetism of [Mn(hfac)$_2$NIT(Ph-m-OPh)], *J. Coord. Chem.*, 2012, **65**, 2683-2691.
5. R. A. A. Cassaro, S. G. Reis, T. S. Araujo, P. M. Lahti, M. A. Novak and M. G. F. Vaz, A Single-Chain Magnet with a Very High Blocking Temperature and a Strong Coercive Field, *Inorg. Chem.*, 2015, **54**, 9381-9383
6. M. G. F. Vaz, R. A. Allão, H. Akpinar, J. A. Schlueter, S. Santos, Jr., P. M. Lahti and M. A. Novak, Magnetic Mn and Co Complexes with a Large Polycyclic Aromatic Substituted Nitronylnitroxide, *Inorg. Chem.*, 2012, **51**, 3138-3145.
7. A. Caneschi, D. Gatteschi, N. Lalioti, C. Sangregorio, R. Sessoli, G. Venturi, A. Vindigni, A. Rettori, M. G. Pini and M. A. Novak, Cobalt(II)-Nitronyl Nitroxide Chains as Molecular Magnetic Nanowires, *Angew. Chem., Int. Ed.*, 2001, **40**, 1760-1763.
8. M. G. F. Vaz, R. A. A. Cassaro, H. Akpinar, J. A. Schlueter, P. M. Lahti and M. A. Novak, A Cobalt Pyrenylnitronylnitroxide Single-Chain Magnet with High Coercivity and Record Blocking Temperature, *Chem. – Eur. J.*, 2014, **20**, 5460-5467.
9. R. A. A. Cassaro, S. G. Reis, T. S. Araujo, P. M. Lahti, M. A. Novak and M. G. F. Vaz, A Single-Chain Magnet with a Very High Blocking Temperature and a Strong Coercive Field, *Inorg. Chem.*, 2015, **54**, 9381-9383.
10. X. Liu, X. Feng, K. R. Meihaus, X. Meng, Y. Zhang, L. Li, J.-L. Liu, K. S. Pedersen, L. Keller, W. Shi, Y.-Q. Zhang, P. Cheng and J. R. Long, Coercive Fields Above 6 T in Two Cobalt(II)–Radical Chain Compounds, *Angew. Chem., Int. Ed.*, 2020, **59**, 10610-10618.
11. R. A. Allão Cassaro, P. M. Lahti, M. G. F. Vaz and M. A. Novak, Lattice Solvent Engineering Improves the Stability of a Cobalt Pyrenylnitronylnitroxide Ferrimagnetic Chain, *Inorg. Chem.*, 2023, **62**, 11248-11255.
12. K. Maryunina, D. Nigomedyanova, V. Morozov, K. Smirnova, G. Letyagin, G. Romanenko, N. Efimov, A. Bogomyakov and V. Ovcharenko, Ferrocenyl-substituted

nitronyl nitroxide in the design of one-dimensional magnets, *Dalton Trans.*, 2024, **53**, 1714-1721.